Biaxial Yielding of Polypropylene/Elastomeric Polyolefin Blends: Effect of Elastomer Content and Thermal Annealing

Laura A. Fasce,[1] Valeria Pettarin,[1] Claudia Marano,[2] Marta Rink,[2] Patricia M. Frontini[1]
[1] *División Polímeros, Instituto de Investigaciones en Ciencia y Tecnología de Materiales, Av. J.B. Justo 4302, B7608FDQ, Mar del Plata, Argentina*

[2] *Dipartamento di Chimica Industriale e Ingegneria Chimica Giulio Natta, Politecnico di Milano, Piazza Leonardo da Vinci 32, 20133, Milano, Italy*

The yield behavior of commercial homopolymer polypropylene modified by elastomeric metallocene-catalyzed polyolefin blends was investigated by carrying out uniaxial tension, uniaxial compression, plane strain compression, and simple shear mechanical tests. Investigation was performed using specimens machined from isotropic compression molded plates. The onset of yielding was determined by means of the residual strain method. Experimental data was fitted according to the two most popular yield criteria in the polymer field—modified Tresca and modified Von Mises criteria. Both criteria provided reasonable predictions of the yield onset locus despite the tendency of polymers to develop crazes under positive hydrostatic pressure. A generalized yield locus based on the modified Von Mises criterion and the Lazzeri and Bucknall relationship was constructed for PP/POE blends. In addition, for one blend composition the effect of the polypropylene matrix crystalline morphology—altered by thermal annealing—was investigated. POLYM. ENG. SCI., 48:1414–1423, 2008. © 2008 Society of Plastics Engineers

INTRODUCTION

Polypropylene (PP) is a thermoplastic polymer with a large number of desirable properties that make it a versatile material, even if its applications are limited by the poor impact strength, especially at low temperatures. Among other strategies used to extend its applications to engineered structures, are the toughening by incorporating a discrete elastomeric phase and the optimization of its crystalline morphology [1–7]. The employment of PP-based materials in structural applications has become widespread and this has led to an increased demand for data regarding their safe limits. Materials based on PP are, for example, widely used for pipes and pressure vessels, and many applications in the automotive industry including bumpers and dashboards, which may also experience multiaxial stress. Studies concerning failure of toughened PP are generally focused on fracture toughness, despite yielding under multiaxial stress can be critical for the structural integrity of engineering components as well.

Predicting the yielding safe limits of a product under combined stresses requires the application of a yield criterion, which, for polymers, must include the effect of hydrostatic pressure on the yield stress [8–10]. Polymeric materials show significant increase in the yield stress with increasing hydrostatic compression; in fact polymers display differences in the compressive and tension yield stress values, up to a relative ratio of the order of 1.3 [11, 12].

The yield stress of rubber toughened semicrystalline polymer blends depends on both the volumetric fraction of rubbery phase and the crystalline morphology of the matrix [7]. This article focus the investigation of the yield behavior of blends of a propylene homopolymer and a metallocenic elastomeric polyolefin having different elastomeric phase content (0–30%) and displaying different crystalline phase morphology induced by thermal annealing. Yield envelopes were determined considering the modified Von Misses and Tresca criteria based on the yield stress values measured under uniaxial tension, uniaxial compression, plane strain compression, and simple shear. Results are interpreted in light of simple phenomenological models available in literature [13] and microstructural considerations.

EXPERIMENTAL

Materials

Rubber-modified PP were prepared by melt blending commercial grades of a PP homopolymer (Cuyolen

Correspondence to: Patricia M. Frontini; e-mail: pmfronti@fi.mdp.edu.ar
Contract grant sponsors: SECyT/MAE bilateral collaboration research programs N°31 Cod. 18C and IT/PA05-MX/122 (MA2).
DOI 10.1002/pen.21107
Published online in Wiley InterScience (www.interscience.wiley.com).

TABLE 1. List of the investigated PP materials and their thermal properties determined by DSC.

Material ID	Description	X_c	$X_{c(PP)}$	T_m (°C)
PPH	Polypropylene homopolymer	47.7	47.7	166
PP/10POE	Mechanical blend of PPH and 10 wt% POE	45.0	50.0	166
PP/20POE	Mechanical blend of PPH and 20 wt% POE	38.6	48.3	166
PP/30POE	Mechanical blend of PPH and 30 wt% POE	34.3	48.9	167
PPH-160	Annealed at 160°C PPH	54.4	54.4	171
PP/10POE-160	Annealed at 160°C PP/10POE	54.0	60.0	172

NX1100 from Petroquímica Cuyo SAIC) and a metallocene-catalyzed polyolefin (ENGAGE POE from Dow Chemicals) [4]. The latter, as reported in the literature [4, 14-16] is an effective impact modifier for PP: it enhances its toughness and decreases its ductile–brittle transition temperature. Three blend compositions were considered, namely 10, 20, and 30 wt% of POE. In a previous paper [4] it was shown that the POE elastomeric phase segregates as almost spherical inclusions having poor adhesion with the continuous PP matrix. Further, particle sizes follow the usual lognormal distribution with mean particle diameters of 0.36, 0.44, and 0.50 μm for 10, 20, and 30 wt% elastomer content, respectively.

Isotropic plates were obtained by compression molding at 200°C and slowly cooled to room temperature to avoid residual thermal stresses generated during cooling.

Besides, plates of PP homopolymer and PP containing 10 wt% of elastomeric polyolefin were further subjected to thermal annealing during 3 h at 160°C. It has been shown that thermal annealing modifies the mechanism of fracture propagation in PP [1, 17, 18] due to the promotion of the interspherulitic crystallization [19].

Thermal properties of materials were determined by differential scanning calorimetry (DSC) analysis. DSC measurements were carried out in a Pelkin Elmer Pyris 1 at a heating rate of 10°C/min from room temperature to 250°C under nitrogen atmosphere. For every performed plate several samples were analyzed and the experimental melting heat (ΔH_m) was evaluated as the average value. Then the overall crystalline fraction, X_c, was calculated by the following equation:

$$X_C = \frac{\Delta H_m}{\Delta H_{m,c}} \tag{1}$$

where $\Delta H_{m,c}$ is the melting heat of a pure crystalline PP material, which was taken as 207.1 J/g [20, 21]. In the case of PP/POE blends, crystallinity of the PP component, $X_{c(PP)}$, was calculated by normalizing ΔH_m by the corresponding PP weight fraction.

Details of the resulting materials along with the abbreviations adopted through this work and their thermal properties are listed in Table 1.

Mechanical Tests

Tests at constant displacement rate so that the initial deformation rate was 0.5 min^{-1} were performed, at room temperature, under uniaxial tension, uniaxial compression, plane strain compression, and simple shear, using an INSTRON 1185 universal testing machine equipped with suitable testing rigs. A measurement of the residual strain was performed on all tested samples 24 h after unloading.

In uniaxial tensile tests, dumb-bell shaped specimens (ASTM D 638) were employed and an extensometer with a gauge length, L_0, of 12.5 mm was used to measure the sample strain during loading. The residual strain was determined by the relative variation of distance between the marks left by the extensometer blades after unloading using an optical microscope with an appropriate scale.

In uniaxial compression tests, the specimen shape was a 10-mm diameter cylinder having a height–diameter ratio of 1. During loading, sample deformation was measured by an extensometer fixed onto the loading plates. The residual strain in the sample after unloading was obtained as the relative variation of sample's height measured by a micrometer.

For both uniaxial tests, the true stress, σ_1, was obtained from load, P, and strain, ε_1, measurements according to the expression:

$$\sigma_1 = \frac{P}{A_0 \cdot (1 - v\varepsilon_1)^2} \tag{2}$$

where A_0 is the specimen's initial cross-sectional area and v is the Poisson's ratio. According to tensile dilatometry measurements previously carried out on the same materials the global volume change was less than 0.35% and the Poisson coefficient was always 0.4 [22].

In plane strain compression tests, prismatic specimens (having thickness, $B = 2$ mm and width, $W = 24$ mm) were used under a die having breadth, $b = 3.5$ mm and width larger than 24 mm. During loading, sample deformation was measured by an extensometer fixed onto the loading plates. Residual strain was obtained as the relative variation of the thickness of the specimen under the die area, which was measured using a caliper. The stresses in the specimen are:

$$\sigma_1 = \frac{P}{W \cdot b} \tag{3}$$

$$\sigma_2 = v\sigma_1 \tag{4}$$

Simple shear tests were performed using testing rigs consisting of a U bolt and a hook which symmetrically shear

TABLE 2. Expressions of significant stresses and strains in terms of principal stresses for the loading configurations used in yield experiments.

	Uniaxial tension	Shear	Uniaxial compression	Plane strain compression
Stress tensor	$\begin{vmatrix} \sigma_1 & 0 & 0 \\ 0 & 0 & 0 \\ 0 & 0 & 0 \end{vmatrix}$	$\begin{vmatrix} \sigma_1 & 0 & 0 \\ 0 & -\sigma_1 & 0 \\ 0 & 0 & 0 \end{vmatrix}$	$\begin{vmatrix} \sigma_1 & 0 & 0 \\ 0 & 0 & 0 \\ 0 & 0 & 0 \end{vmatrix}$	$\begin{vmatrix} \sigma_1 & 0 & 0 \\ 0 & \nu\sigma_1 & 0 \\ 0 & 0 & 0 \end{vmatrix}$
	$(\sigma_1 > 0)$	$(\sigma_1 > 0)$	$(\sigma_1 < 0)$	$(\sigma_1 < 0)$
Strain tensor	$\begin{vmatrix} \varepsilon_1 & 0 & 0 \\ 0 & -\nu\varepsilon_1 & 0 \\ 0 & 0 & -\nu\varepsilon_1 \end{vmatrix}$	$\begin{vmatrix} \varepsilon_1 & 0 & 0 \\ 0 & -\varepsilon_1 & 0 \\ 0 & 0 & 0 \end{vmatrix}$	$\begin{vmatrix} \varepsilon_1 & 0 & 0 \\ 0 & -\nu\varepsilon_1 & 0 \\ 0 & 0 & -\nu\varepsilon_1 \end{vmatrix}$	$\begin{vmatrix} \varepsilon_1 & 0 & 0 \\ 0 & 0 & 0 \\ 0 & 0 & -\frac{\nu}{1-\nu}\varepsilon_1 \end{vmatrix}$
	$(\varepsilon_1 > 0)$	$(\varepsilon_1 > 0)$	$(\varepsilon_1 < 0)$	$(\varepsilon_1 < 0)$
Maximum shear stress (τ_T)	$\frac{\sigma_1}{2}$	σ_1	$-\frac{\sigma_1}{2}$	$-\frac{\sigma_1}{2}$
Octahedral shear stress (τ_{oct})	$\frac{\sqrt{2}}{3}\sigma_1$	$\frac{\sqrt{6}}{3}\sigma_1$	$-\frac{\sqrt{2}}{3}\sigma_1$	$-\frac{\sqrt{2}}{3}\sigma_1\sqrt{1+\nu^2-\nu}$
Hydrostatic mean stress (σ_m)	$\frac{\sigma_1}{3}$	0	$\frac{\sigma_1}{3}$	$\frac{\sigma_1(1+\nu)}{3}$

two zones of a prismatic sample following [23, 24]. The two sheared zones have a cross-sectional area $A_0 = 6 \times 12$ mm^2 and a width $W = 2$ mm. Residual shear strain was measured as the ratio between the displacement in the loading direction and the specimen width in the sheared zone, W. The displacement was measured with the aid of a microscope as the deviation of a straight line slightly scratched on the specimen surface before testing. The stresses field of the specimen is given by:

$$\sigma_1 = \left(\frac{P}{2A_0}\right) \tag{5}$$

$$\sigma_2 = -\sigma_1 \tag{6}$$

Table 2 reports the relevant stress and strain for the used test configurations that are sketched in Fig. 1.

Yield Onset Determination

Yield is generally defined as the point after which a material is permanently deformed. The yield stress of polymers is identified in several ways (see for example [25]) and all are, in essence, arbitrary. Some of them define the maximum load as the yield load, and both the nominal stress and the true stress are called the yield stress. The engineering approach proposes an offset-method [25], which could be used if the load displacement curve does not show a maximum, but it would be open to debate whose percent offset is reasonable. In any case, none of these methods is adequate for polymeric materials because of their viscoelastic behavior; a permanent deformation is not easy to identify. The so-called residual strain method has been proposed and successfully applied to determine yield onset for amorphous and semicrystalline polymers [23, 26–29].

Following this method in the present work, for each material and test configuration, a series of identical specimens were loaded up to different strain levels and, after unloading, their residual strains were measured. Residual strains were then plotted as a function of applied strains and linearly back extrapolated to zero residual strain to determine the strain (ε_y) at which permanent deformation (yield) onsets. The stress corresponding to this strain on the relevant stress–strain curve is the yield stress (σ_y). An average of the σ_y values arising from at least five stress–strain curves was taken as the yield stress.

Yield Analysis

The modified Tresca criterion is one of the early criteria proposed to describe the yielding of polymers. It can be formulated as (see for example in [13]):

$$\tau_T = \tau_T^o - \mu_T \cdot \sigma_m \tag{7}$$

in which τ_T is the maximum shear stress, expressed in terms of the principal stresses as:

$$\tau_T = \frac{1}{2}\left|\sigma_i - \sigma_j\right|_{max} \tag{8}$$

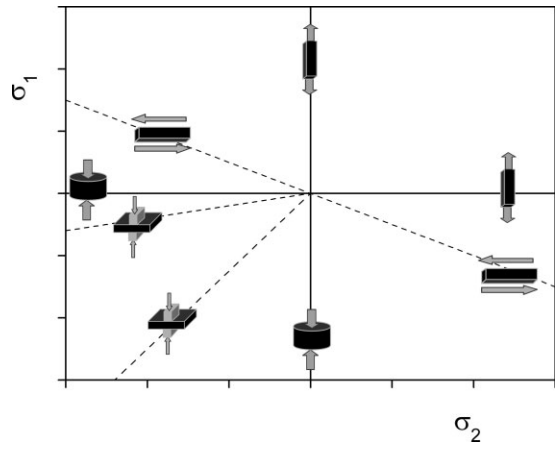

FIG. 1. Schematic of loading configurations used in the yield experiments.

 DOI 10.1002/pen

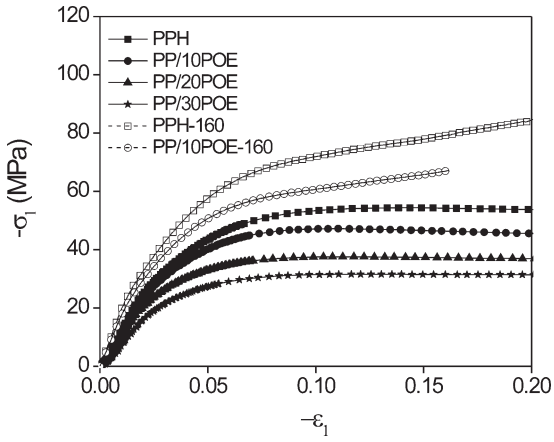

FIG. 2. Typical stress–strain curves under uniaxial compression.

σ_m, is the hydrostatic component of the stress tensor, given by:

$$\sigma_m = \frac{1}{3}(\sigma_1 + \sigma_2 + \sigma_3) \tag{9}$$

and the parameters τ_T° and μ_T are material properties.

The modified Von Mises criterion, which has been widely used to describe the yielding behavior of several amorphous and semicrystalline polymers [13, 24, 30–33], can be expressed as:

$$\tau_{oct} = \tau_{oct}^o - \mu_{VM} \cdot \sigma_m \tag{10}$$

where τ_{oct} is the octahedral shear stress:

$$\tau_{oct} = \frac{1}{3} \cdot \left[(\sigma_1 - \sigma_2)^2 + (\sigma_1 - \sigma_3)^2 + (\sigma_2 - \sigma_3)^2\right]^{1/2} \tag{11}$$

and the parameters τ_{oct}^o and μ_{VM} are material properties.

For both criteria, the limiting value, i.e., the distortional strain energy density in the case of modified Von Mises and the maximum shear stress for modified Tresca, is linearly dependent on pressure. The parameters τ_{oct}^o and τ_T° are the critical octahedral shear stress and shear stress under zero pressure, respectively. The coefficients μ_{VM} and μ_T quantify the yield stress sensitivity to pressure.

From the yield stress values measured under different stress states, it was possible to assess which of the two proposed criteria is more adequate [23].

The parameters of the modified Tresca and modified Von Mises criteria were determined by fitting—using the minimum least squares method—*Eqs. 7* and *10* to all available yield data expressed in terms of their octahedral shear stress or maximum shear stress as a function of hydrostatic mean stress (Table 2).

RESULTS

Overall Behavior of Tested Specimens

Uniaxial tensile specimens of the two grades of propylene homopolymer (PPH and PPH-160) fractured right after yielding, displaying practically brittle behavior. Under the other stress states considered their behavior turned out to be ductile.

The blends always behaved in a completely ductile manner displaying very little strain softening.

The annealed grades (PPH-160 and PP/10POE-160), instead, showed a remarkable tendency to strain harden without previous strain softening and larger overall stress values. Strain hardening after yielding is especially evident under uniaxial compression as can be seen in the stress–strain curves shown in Fig. 2.

Yield Stress Determination

Preliminary recovery experiments in which the residual strain after unloading was measured as a function of recovery time at room temperature were performed. As an example, in Fig. 3, the strain recovery of compressed samples is shown for two of the studied materials. It can be observed that the residual strain tends to an asymptotic value, which irrespectively of the material, can be thought to be reached after a recovery time of 1 day (1440 min).

Referring to literature [23, 27, 34], the recovery of the residual strain after unloading is due to the time-dependent recovery of the viscoelastic strain component. When the asymptotic value of the residual strain is reached, the viscoelastic strain component has completely recovered and the residual strain is equal to the plastic strain component. In our case, the plastic strain was thus measured as the residual strain at a recovery time of 1 day after unloading.

The general yield stress determination procedure is exemplified in Fig. 4 while the values of stresses at yield onset are reported in Table 3 together with the relevant standard deviations. No particular feature can be identified on the stress–strain curve at the onset of yielding (see Fig. 4).

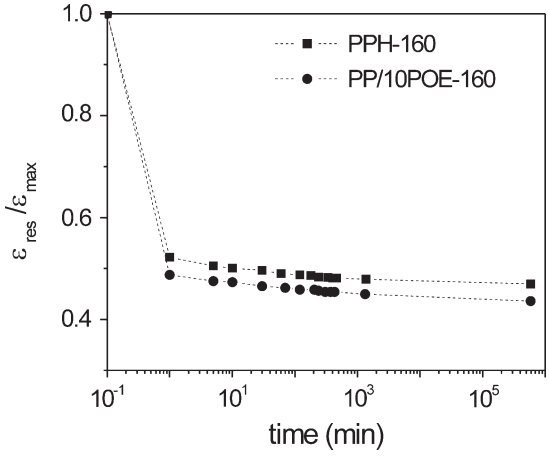

FIG. 3. Normalized residual strains as a function of recovery time at room temperature after unloading for uniaxially compressed samples.

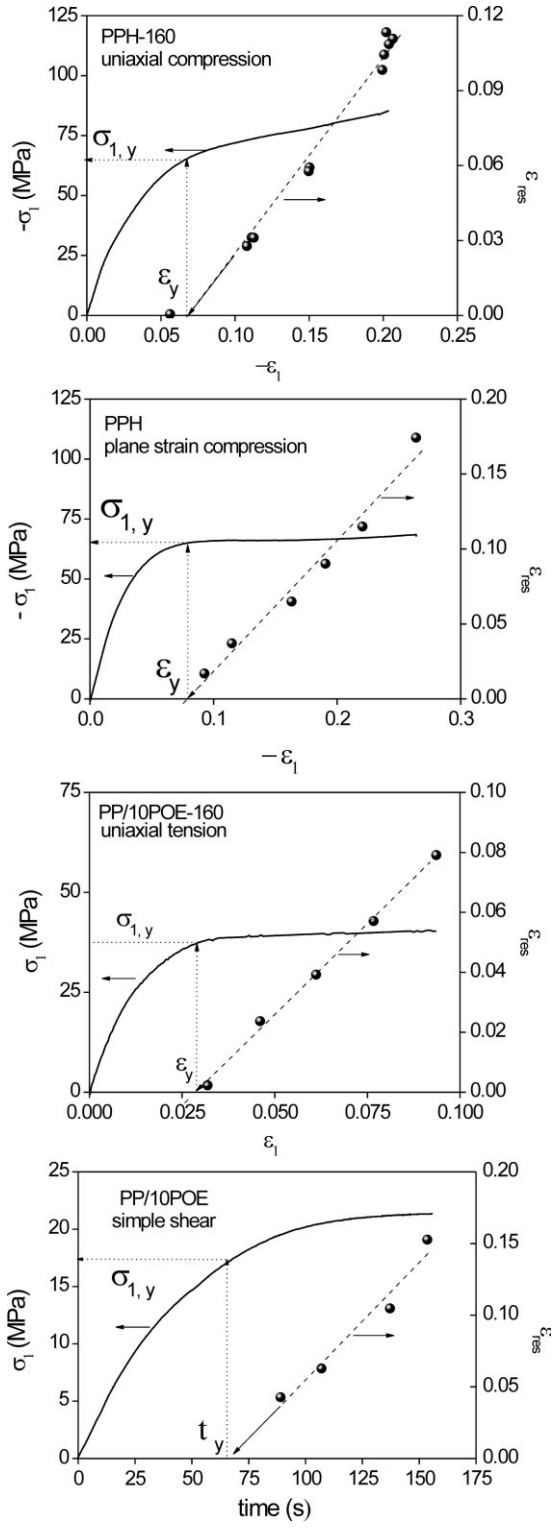

FIG. 4. Examples of yield stress determination using the "residual strain method" from the stress–strain curves and residual strain-applied strain plots.

In the cases of PPH and PPH-160 subjected to uniaxial tension, the yield stress was assumed to be the maximum stress value since the residual strain method could not be applied because specimens displayed practically brittle fracture.

DISCUSSION

Yield Criteria Parameters

Figure 5 plots the experimental octahedral shear stress (Fig. 5a) and the maximum shear stress (Fig. 5b) as a function of hydrostatic mean stress for each material and Table 4 summarizes the criteria parameters obtained by fitting experimental data points. In Table 4, bold characters are adopted for the values of the parameters relevant to the yield criterion, which is more suitable for each material as judged from the linear regression coefficient (R^2). Actually, there is a no clear reason to choose one model rather than the other for the studied PP polymers in the "as-molded" state (i.e. PPH and PP/POE blends). On the contrary, modified Tresca criterion gives better prediction of the yield locus of the annealed PP-based polymers (PPH-160, PP/10POE-160). These materials show a deformation behavior different from that of the PP polymers in the "as-molded" state, as it was described in the Overall Behavior of Tested Specimens section.

It is known that brittle fracture of PP is preceded by crazing [7, 35, 36]. Crazing phenomena is generally described by other criteria [37–40], which take into account that it occurs only under stress states having a positive hydrostatic mean stress as in the case of uniaxial tension [9, 41]. Consistently, a second fitting procedure was performed considering all data but tensile yield stress values. The relevant parameters obtained are presented in Table 5. It can be seen that this second procedure led in practice, to the same yielding locus predicted by the fitting procedure in which all data points were used. This fact suggests that under uniaxial tension either crazing or shear yielding may occur at similar critical stress values and that the yielding locus is not practically affected by crazing.

Effect of Elastomer Content

In Fig. 6 the yield stress values of PP/POE blends are plotted versus the elastomer volume fraction. As expected, yield stress gradually decreases with increasing elasto-

TABLE 3. Stresses at yield onset under different stress states for PP polymers expressed in MPa.

Material ID	Uniaxial tensile	Uniaxial compression	Plane strain compression	Simple shear
PPH	36.0±1.5	51.3±1.0	64.3±0.5	22.8±1.0
PP/10POE	30.0±0.6	46.5±0.3	55.4±0.7	17.9±1.4
PP/20POE	25.2±0.7	36.2±0.6	42.9±0.9	16.0±0.3
PP/30POE	21.4±0.8	29.0±1.0	33.9±0.5	14.0±1.5
PPH-160	42.7±3.1	65.7±0.5	68.7±3.0	24.8±0.5
PP/10POE-160	35.3±1.4	58.1±0.8	57.3±0.8	18.9±0.1

The corresponding standard deviations are also reported.

DOI 10.1002/pen

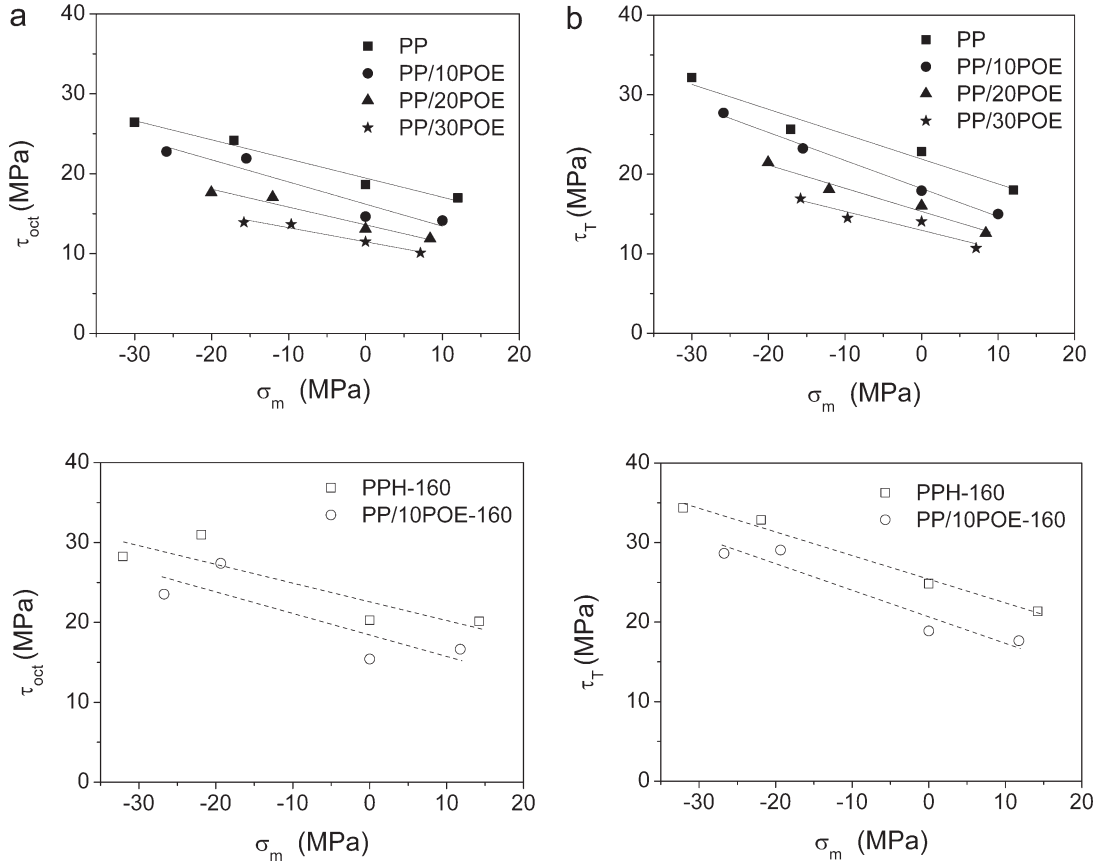

FIG. 5. (a) Octahedral shear stress versus hydrostatic stress; (b) Maximum shear stress versus hydrostatic stress. Dots are experimental values while lines are the corresponding linear regressions.

meric content in all stress states considered [42, 43]. This occurs because the rubber particles have very low shear modulus compared to PP and thus load is mainly borne by the PP matrix [44].

The dependence of the tensile yield stress on elastomer volume fraction in rubber-modified PP systems was described by the following simple equation [44]:

$$\sigma_y = \sigma_{matrix}(1 - 1.375\phi) \tag{12}$$

where σ_y and σ_{matrix} are the yield stresses of the blend and the matrix, respectively, and ϕ is the volume fraction of the dispersed phase. Lazzeri and Bucknall previously proposed this equation for rubber-toughened polymethylmethacrylate (PMMA) under uniaxial compression [45]. It was also shown to be suitable for other stress states provided no particle cavitation occurs.

In the case of PP/POE blends (Fig. 6a) and annealed materials, PPH-160 and PP/10POE-160 (Fig. 6b), a good agreement between experimental data and the predictions of *Eq. 12* is found. For the yield stress (σ_y) predictions, according to *Eq. 12* (solid lines in Fig. 6), an average value of the PP matrix yield stress (σ_{matrix}) was used for each stress state: it was calculated as the mean values obtained for σ_{matrix} applying *Eq. 12* to every single experimental yield stress value of each blend.

TABLE 4. Values of yield criteria parameters obtained by fitting all available yield stresses.

	Von Misses			Tresca		
Material	τ^o_{oct} (MPa)	μ_{VM}	R^2	τ^o_T (MPa)	μ^T	R^2
PPH	19.5	0.24	0.98	21.9	0.31	0.96
PP/10POE	16.2	0.28	0.92	18.2	0.35	0.99
PP/20POE	13.6	0.22	0.96	15.3	0.29	0.94
PP/30POE	11.5	0.18	0.96	13.0	0.24	0.89
PPH-160	22.6	0.23	0.78	25.4	0.30	0.99
PP/10POE-160	18.4	0.27	0.70	20.7	0.33	0.92

TABLE 5. Values of yield criteria parameters obtained by fitting all yield stresses but uniaxial tensile.

	Von Misses			Tresca		
Material	τ^o_{oct} (MPa)	μ_{VM}	R^2	τ^o_T (MPa)	μ^T	R^2
PPH	19.0	0.26	0.98	22.1	0.30	0.91
PP/10POE	15.3	0.33	0.90	17.8	0.38	0.99
PP/20POE	13.4	0.24	0.92	15.7	0.26	0.91
PP/30POE	11.7	0.16	0.91	13.7	0.17	0.76
PPH-160	21.3	0.29	0.71	25.1	0.31	0.97
PP/10POE-160	16.5	0.37	0.69	19.4	0.40	0.91

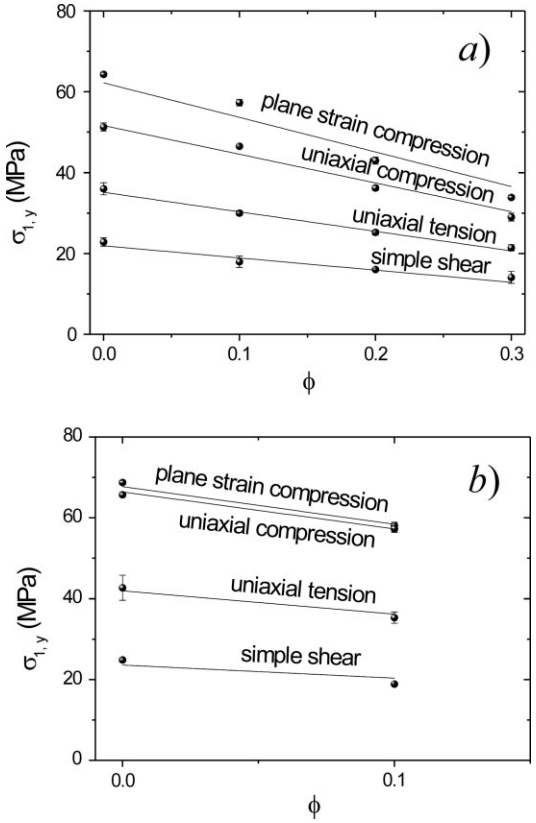

FIG. 6. Yield stress as a function of elastomer volume fraction in (a) PP/POE blends and (b) annealed materials (PPH-160, PP/10POE-160). Experimental data and predictions by *Eq. 12* are represented by dots and solid lines, respectively.

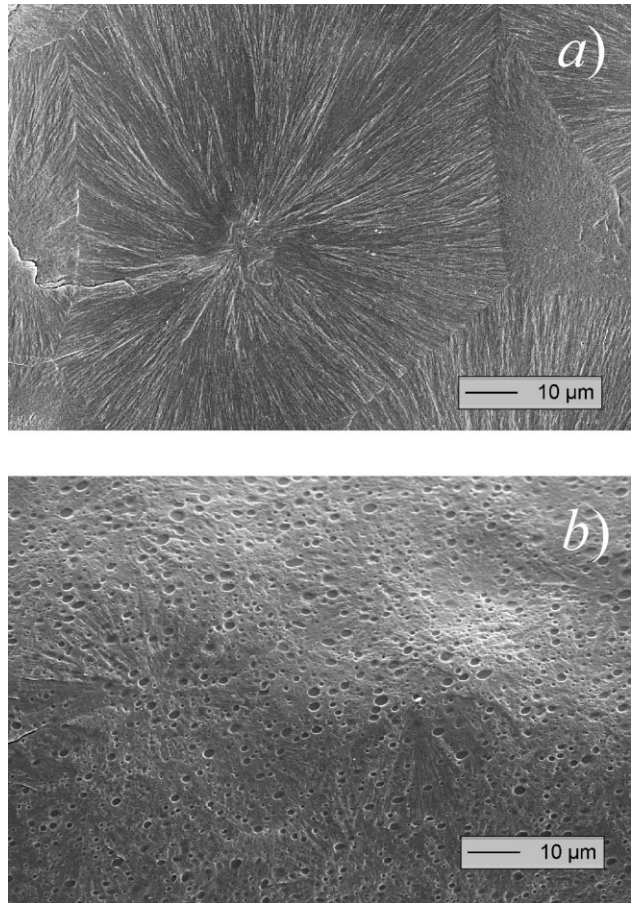

FIG. 7. SEM micrographs of (a) PPH and (b) PP/10POE after etching with permanganic acid solution.

The good agreement between experimental data and the data predicted using *Eq. 12* indicates that:

i. The morphology of the PP matrix is not altered by the addition of the elastomeric POE phase. This fact was confirmed by DSC analysis and SEM inspection. Both the melting temperature, T_m, and the PP crystallinity, $X_{c(PP)}$, are practically constant irrespective of elastomer content in the PP/POE blends as shown in Table 1. Moreover, the spherulitic structure of the homopolymer PP was observed also in the blends. As an example, in Fig. 7, micrographs of PPH and PP/10POE after removal of elastomeric particles are compared. The results obtained are in agreement with others in literature pointing out that the presence of rubber particles in a PP matrix normally does not affect its crystalline morphology [36, 44, 46, 47].
ii. The investigated blends do not show a yield stress dependency upon the size of the POE particles, which is indeed different in the three blends studied. The same behavior was found for other rubber modified polymeric systems like PP/SEBS [48], PP/EPDM [49], nylon-rubber blends [50, 51], and rubber-toughened PMMA [52]. When deformation of rubber-toughened polymers is governed by shear yielding mechanism, the yield behavior appears to be insensitive to the sizes of the particles, provided, they are large enough to constitute a completely separate phase and have sharp interfaces [53, 54].

In Fig. 8 the values of the Von Mises yield criterion parameters, τ°_{oct} and μ_{VM}, are plotted versus the elastomeric volume fraction together with the τ°_{oct} prediction (solid lines in Fig. 8) obtained by applying *Eq. 12* as:

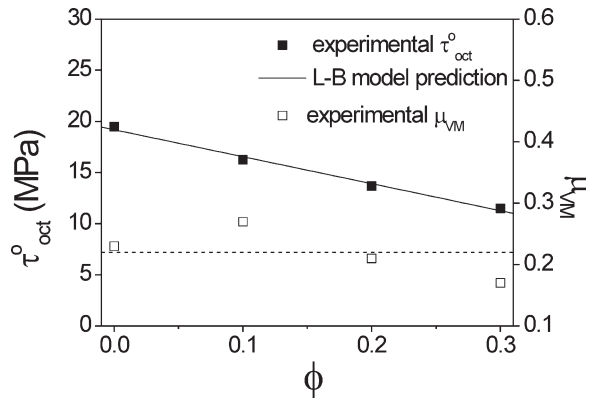

FIG. 8. Modified Von Mises criterion parameters as a function of elastomer volume fraction in PP/POE blends.

DOI 10.1002/pen

$$\tau^{o}_{oct} = \tau^{o}_{oct_{matrix}}(1 - 1.375\phi) \quad (13)$$

For $\tau^{o}_{oct_{matrix}}$ a value of 19.1 MPa was calculated, as previously done, as the mean of the $\tau^{o}_{oct_{matrix}}$ obtained by applying *Eq. 13* using the experimental values of τ°_{oct} for PPH and PP/POE blends reported in Table 4.

The yield stress pressure sensitivity coefficient, μ_{VM}, does not show any trend as rubber content increases, being practically the same for all of the "as-molded" blends. Therefore, a sole value was assumed to describe all the systems equal to the average (0.22).

Figure 9 shows the yield envelope obtained according to *Eq. 10* with $\tau^{\circ}_{oct} = 19.1$ MPa and $\mu_{VM} = 0.22$, together with the experimental yield points of PP/POE blends, each normalized by the relevant factor $1/(1 - 1.375\phi)$. This generalized modified Von Mises envelope well describes the yield behavior of as-molded PP/POE blends.

Effect of Annealing

Besides promoting strain hardening (see Overall Behavior of Tested Specimens section), annealing at 160°C increases yield stress values and also slightly enhances compression to tensile yield stress ratio for both PP and its blend with 10 wt% POE (Table 3).

Larger yield stress values are consistent with the moderate enhancement of crystalline fraction and lamellar thickness [55, 56], revealed by the increase in ΔH and T_m values, respectively (Table 1) [57].

Yielding and pos-yielding deformation processes in semicrystalline polymers are associated with irreversible deformations such as coarse slip and fragmentation of lamellar blocks [25]. From a microscopic point of view, hardening results from the presence of obstacles, which oppose the growth of the plastic process [58]. In addition to lamellar thickening, annealing operates through a partial melting and recrystallization process, growth of thin

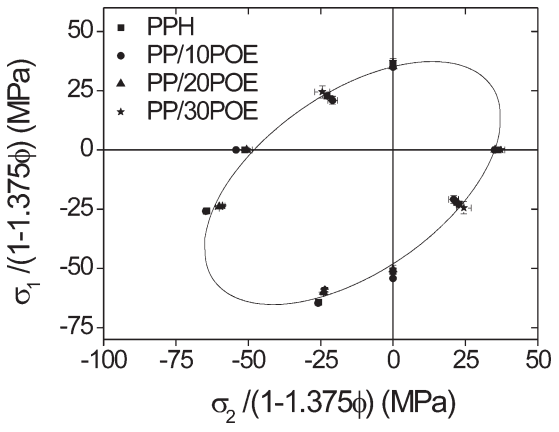

FIG. 9. Generalized yield locus for PP/POE blends according to the modified Von Misses criterion. Experimental points are reported normalized dividing the yield stress by (1–1.375ϕ).

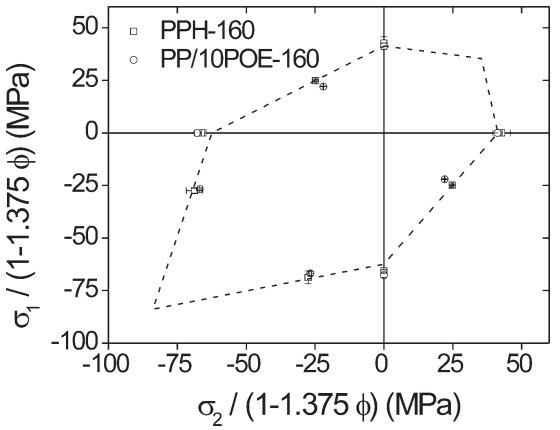

FIG. 10. Generalized yield locus for annealed materials according to the modified Tresca criterion. Experimental points of PP/10POE-160 are reported normalized dividing the yield stress by (1–1.375ϕ).

crystallites into the amorphous zones, and rearrangement of uncrystallized polymer chains [18] yielding to a more physically interconnected network. When lamellar fragmentation prevails, like in less organized PP systems (i.e. the as-molded materials), the material strain softens: the nominal stress drop occurs just past the yield point due to the failure and disconnection of the lamellas and remains stationary while the tie molecules are pulled out from the fragmented lamella and become part of the amorphous layers. Conversely, in more interconnected systems (i.e. the annealed materials), lamellae remains linked by tie molecules and aligned parallel to the deformation direction beyond the yield point exhibiting strain hardening due to molecular network orientation [59, 60].

As for the parameters of the modified Tresca criterion (τ^{o}_{T} and μ_T) which has been shown to better describe the yield behavior of annealed materials, τ^{o}_{T} increases with thermal treatment consistently with the increase in σ_y while the yield stress pressure sensitivity coefficient slightly increases with annealing (Table 4).

In Fig. 10 the relevant envelope of the modified Tresca criterion of the PPH-160 is constructed using *Eq. 7* with $\tau^{o}_{T} = 25.4$ MPa and $\mu_T = 0.30$. Yield data points of PP/10POE-160 were normalized assuming *Eq. 12* and then plotted along with the PPH-160 values in Fig. 10. It seems that the yield behavior of annealed blends could also be described by a generalized yield locus based on the modified Tresca criterion, by considering:

$$\tau^{o}_{T} = \tau^{o}_{T_{matrix}}(1 - 1.375\phi) \quad (14)$$

where $\tau^{o}_{T_{matrix}}$ is assumed to be equal to the value determined for the annealed PP (25.4 MPa).

CONCLUSIONS

The yield behavior of propylene homopolymer/elastomeric metallocene-catalyzed polyolefin blends was

studied through constant strain rate tests performed on flat samples under different loading configurations.

Our results show that practically either modified Von Mises or modified Tresca criteria provide reasonable predictions of the yield onset of isotropic homogeneous propylene homopolymer as well as its blends with elastomeric polyolefin. Moreover, both criteria well describe the yield behavior of PP polymers despite their tendency to craze when the hydrostatic component of the stress tensor is positive.

Further, it was shown that blends' critical yield stress follows the linear decreasing trend with elastomer content predicted by Lazzeri and Bucknall equation [45]. This result is consistent with the hypothesis of poor adhesion between POE particles and PP matrix and with a yield stress insensitive to particle size, since the blends have different mean particle size values.

A generalized yield locus was constructed for PP/POE blends based on the modified Von Mises criterion and Lazzeri and Bucknall equation. This appealing finding supports the additional idea that the morphology of the PP matrix is not altered by the presence of elastomeric POE particles.

Modified Tresca criterion was found to better describe the yield behavior of annealed systems. They show a different yielding deformation behavior as a consequence of the different microstructure developed: under uniaxial compression they strain harden after yielding while the "as-molded" materials strain soften. This suggests that the acting deformation micromechanisms differ from those characteristic of the "as-molded" materials.

ACKNOWLEDGMENTS

The authors thank Prof. G. Michler and Dipl.-Phys. S. Henning from Martin-Luther University for performing SEM experiments.

REFERENCES

1. P.M. Frontini and A. Fave, *J. Mater. Sci*., **30**, 2446 (1995).
2. J.M. Hodgkinson, A. Savadori, and J.G. Williams, *J. Mater. Sci*., **18**, 2319 (1986).
3. W. Jiang, S.C. Tjong, and R.K.Y. Li, *Polymer*, **41**, 3479 (2000).
4. L.A. Fasce, P.M. Frontini, S.-C. Wong, and Y.-W. Mai, *J. Polym. Sci. Part B: Polym. Phys*., **42**, 1075 (2004).
5. J. Karger-Kocsis, *Compos. Sci. Technol*., **48**, 273 (1993).
6. T. Inoue and T. Suzuki, *J. Appl. Polym. Sci*., **59**, 1443 (1996).
7. J.Z. Liang and R.K.Y. Li, *J. Appl. Polym. Sci*., **77**, 409 (2000).
8. R. Raghava, R.M. Caddell, and G.S.Y. Yeh, *J. Mater. Sci*., **8**, 225 (1973).
9. S.S. Sternstein and L. Ongchin, *ACS Polym Prepr*., **10**, 1117 (1969).
10. J.C. Bauwens, *J. Polym Sci*., **8**, 893 (1970).
11. R.M. Caddell, R.S. Raghava, and A.G. Atkins, *Mater. Sci. Eng*., **13**, 113 (1974).
12. W. Hu and Z.R. Wang, *Comput. Mater. Sci*., **32**, 31 (2005).
13. A.J. Kinloch and R.J. Young, *Fracture Behavior of Polymers*, Applied Science Publishers, London Essex, 107 (1983).
14. H.C. Silvis, R.C. Cieslinski, D.J. Murray, and S.P. Chum, *Proceedings of the International Congress and Exposition on Advances in Automotive Plastic Components and Technology*, Detroit, 69 (1995).
15. A.L.N. Silva, M.I.B Tavares, D.R. Politano, F.M.B. Coutinho, and M.C.G. Rocha, *J. Appl. Polym. Sci*., **66**, 2005 (1997).
16. L.A. Fasce and P.M. Frontini, *J. Macromol. Sci., Phys*., **41**, 1231 (2002).
17. M.L. Maspoch, D. Ferrer, A. Gordillo, O.O. Santana, A.B. Martinez, *J. Appl. Polym. Sci*., **73**, 177 (1999).
18. R. Greco and G. Ragosta, *J. Mater. Sci*., **23**, 4171 (1988).
19. J. Varga, *J. Mater. Sci*., **27**, 2557 (1992).
20. H.S. Bu, S.Z.D. Cheng, and B. Wunderlich, *Makromol. Chem. Rapid Commun*., **9**, 76 (1988).
21. J. Brandrup, E.H. Immergut, and E.A. Grukle, *Polymer Handbook*, Wiley, New York (1999).
22. L.A. Fasce, *Mechanical and Fracture Characterization of PP/POE Blends*. PhD Thesis on Materials Science, University of Mar del Plata, Argentina (2002).
23. R. Quinson, J. Perez, M. Rink, and A. Pavan, *J. Mater. Sci*., **31**, 4387 (1996).
24. R. Quinson, J. Perez, M. Rink, and A. Pavan, *J. Mater. Sci*., **32**, 1371 (1997).
25. I. Ward and D. Hadley, *An Introduction to the Mechanical Properties of Solid Polymers*, Wiley, England (1993).
26. J. Rose, R.A. Duckett, and I.M. Ward, *J. Mater. Sci*., **30**, 5328 (1995).
27. C. Marano and M. Rink, *Polymer*, **42**, 2113 (2001).
28. C. Marano and M. Rink, *Mech. Time-Depend. Mater*., **10**, 173 (2006).
29. A. Pegoretti, A. Guardini, C. Migliaresi, and T. Ricco, *Polymer*, **41**, 1857 (2000).
30. A.J. Lesser and R.S. Kody, *J. Polym. Sci., Part B: Polym. Phys*., **35**, 1611 (1997).
31. J.S.N. Sultan and F.J. McGarry, *Polym. Eng. Sci*., **13**, 29 (1973).
32. L.M. Carapellucci and A.F. Yee, *Polym. Eng. Sci*., **26**, 920 (1986).
33. L.E. Asp, L.A. Berglund, and R. Talreja, *Compos. Sci. Technol*., **56**, 1291 (1996).
34. A. Pegoretti, A. Guardini, C. Migliaresi, and T. Ricco, *J. Appl. Polym. Sci*., **78**, 1664 (2000).
35. I. Narisawa, *Polym. Eng. Sci*., **27**, 41 (1987).
36. C.J. Chou, K. Vijayan, D. Kirby, A. Hiltner, and E. Baer, *J. Mater. Sci*., **23**, 2521 (1988).
37. R.J. Oxborough and P.B. Bowen, *Philos. Mag*., **28**, 547 (1973).
38. S.S. Sternstein and F.A. Myers, *J. Macromol. Sci. Phys*., **8**, 539 (1973).
39. M. Ishikawa and I. Narisawa, *J. Mater. Sci*., **18**, 1947 (1983).

40. C.B. Bucknall, *Proceedings of the 13th International Conference on Deformation, Yield and Fracture of Polymers*, Kerkrade, The Netherlands, 77 (2006).
41. J.T. Woods and H.G. Delorenzi, *Polym. Eng. Sci.*, **33**, 1431 (1993).
42. B. Pukánszky, F. Tudos, A. Kalló, and G. Bodor, *Polymer*, **30**, 1407 (1989).
43. A. van der Wal, R. Nijhof, and R.J. Gaymans, *Polymer*, **40**, 6031 (1999).
44. S.M. Zebarjad, R. Bagheri, S.M. Seyed Reihani, and A. Lazzeri, *J. Appl. Polym. Sci.*, **90**, 3767 (2003).
45. A. Lazzeri and C.B. Bucknall, *Polymer*, **36**, 2895 (1995).
46. L. D'Orazio, C. Mancarela, E. Martuscelli, and G. Sticotti, *J. Mater. Sci.*, **26**, 4033 (1991).
47. J. Lu, G.X. Wei, H.J. Sue, and J. Chu, *J. Appl. Polym. Sci.*, **76**, 311 (2000).
48. F. Stricker, Y. Thomann, and R. Mülhaupt, *J. Appl. Polym. Sci.*, **68**, 1891 (1998).
49. A. van der Wal, R. Nijhof, R.J. Gaymans, *Polymer*, **40**, 6057 (1999).
50. R.J.M. Borggreve, R.J. Gaymans, J. Schuijer, and J.F.I. Housz, *Polymer*, **28**, 1489 (1987).
51. R.J.M. Borggreve, R.J. Gaymans, and A.R. Luttmer, *Makromol. Chem. Macromol. Symp.*, **16**, 195 (1988).
52. J.M. Gloaguen, P. Hein, P. Gaillard, and J.M. Lefebvre, *Polymer*, **33**, 4741 (1992).
53. C.B. Bucknall, "Deformation Mechanisms in Rubber-Toughened Polymers," in *Polymer Blends, Vol. 2, Performance*, D.R. Paul and C.B. Bucknall Eds., Wiley, New York, 83 (2000).
54. W.H. Lee, "Toughened Polymers," in *Polymer Blends and Alloys*, M.J. Folkes and P.S. Hope, Eds., Chapman & Hall, Glasgow, 163 (1993).
55. B.A.G. Schrauwen, *Deformation and Failure of Semicrystalline Polymer Systems: Influence of Micro and Molecular Structure*, PhD Thesis, Technische Universiteit, Eindhoven (2003).
56. K.-H. Nitta, *Comput. Theor. Polym. Sci.*, **9**, 19 (1999).
57. P. Maiti, M. Hikosaka, K. Yamada, A. Toda, and F. Gu, *Macromolecules*, **33**, 9069 (2000).
58. L. Cangémi and Y. Meimon, *Oil Gas Sci. Technol.*, **56**, 555 (2001).
59. A.D. Drozdov and J. de C. Christiansen, *Int. J. Solids Struct.*, **40**, 1337 (2003).
60. K.-H. Nitta and M. Takayanagi, *J. Polym. Sci. Part B: Polym Phys.*, **37**, 357 (1999).